

# Neutronics Analyses for Shield Upgrading of the Compact Neutral Particle Analyzer for LHD Deuterium Plasma Experiments<sup>\*)</sup>

Takeo NISHITANI<sup>1)</sup>, Tetsuo OZAKI<sup>1)</sup>, Kenji SAITO<sup>1)</sup>, Shuji KAMIO<sup>1)</sup>, Kunihiro OGAWA<sup>1,2)</sup>, Mitsutaka ISOBE<sup>1,2)</sup> and Masaki OSAKABE<sup>1,2)</sup>

<sup>1)</sup>National Institute for Fusion Science, National Institutes of Natural Sciences, 322-6 Oroshi-cho, Toki 509-5292, Japan

<sup>2)</sup>SOKENDAI (The Graduate University for Advanced Studies), 322-6 Oroshi-cho, Toki 509-5292, Japan

(Received 18 December 2018 / Accepted 4 February 2019)

The Compact Neutral Particle Analyzer (CNPA) is an E//B type neutral particle energy analyzer using permanent magnets. CNPA is installed on the diagnostic platform and connected to the outside horizontal port. Based on the preliminary shielding design, 15 cm thick borated polyethylene shields were installed before the fast deuterium plasma campaign. However, neutron induced noises could not be ignored in plasmas with the neutron emission rate higher than  $\sim 1 \times 10^{14}$  n/s. We carried out the detailed neutronics analyses for the original neutron shield by using the MCNP6 code, which takes into account the detailed structure. The neutron streaming from the beam inlet and the penetration of the bulk shield are approximately 60% and 40% contribution to the neutron flux at the detector array, respectively. Consequently, 5 cm borated polyethylene plates are added to the bulk shield and an extension shield of borated polyethylene cylinder shield with 20 cm in diameter and 35 cm in length is added around the beam inlet, where the neutron flux is expected to be  $1.9 \times 10^6$  n/cm<sup>2</sup>·s at the detector array for the plasma with the neutron emission rate of  $1.9 \times 10^{16}$  n/s.

© 2019 The Japan Society of Plasma Science and Nuclear Fusion Research

Keywords: compact neutral particle analyzer, shielding design, MCNP, neutron streaming, deuterium plasma, LHD

DOI: 10.1585/pfr.14.3405048

## 1. Introduction

The deuterium plasma experiment was initiated in March 2017 in the Large Helical Device (LHD) [1]. The licensed annual neutron budget is  $2.1 \times 10^{19}$  neutrons/year. The maximum neutron production rate is expected to be  $1.9 \times 10^{16}$  n/s [2]. In such a radiation environment, many diagnostic and control components, such as a programmable logic controller (PLC) and detectors, have possibilities of radiation induced noises, errors, and damage. Therefore, relocation to the basement or the peripheral region of the torus hall, and shielding was undertaken for control and diagnostic systems before the first deuterium plasma campaign. Some diagnostic equipment must remain in the torus hall, mainly because that equipment must face the plasma directly. Radiation shielding is required for such diagnostics equipment in order to avoid radiation induced noises and errors. In this paper, shielding design for the compact neutral particle analyzer (CNPA) [3, 4] is presented as one such example. Before the first deuterium plasma campaign, 15 cm thick borated polyethylene shields were installed based on the preliminary neutronics design. However, it was found that neutron induced noises could not be ignored in plasmas with the neutron emission rate higher than  $\sim 1 \times 10^{14}$  n/s. This paper concentrates on

the neutronics analyses for the original neutron shield, and the upgraded shielding design to improve the shielding performance.

## 2. Compact Neutral Particle Analyzer (CNPA)

The Compact Neutral Particle Analyzer (CNPA) is an E//B type neutral particle energy analyzer using permanent magnets as shown in Fig. 1.

This analyzer was developed by the Ioffe Institute, Russia [4]. Neutral particles from the plasma are ionized on an electron stripping foil. After the ionization, the ion orbits are bent by the permanent magnet, and those ions are detected by the channeltron array. The incident neutral particle energy is analyzed by the position of the channel-

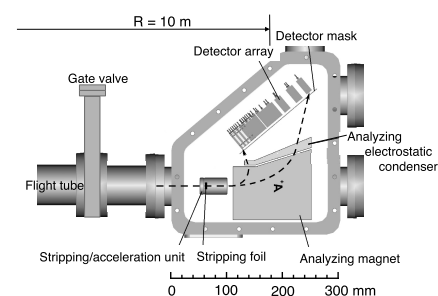


Fig. 1 Schematic view of the CNPA.

author's e-mail: nishitani.takeo@nifs.ac.jp

<sup>\*)</sup> This article is based on the presentation at the 27th International Toki Conference (ITC27) & the 13th Asia Pacific Plasma Theory Conference (APPTC2018).

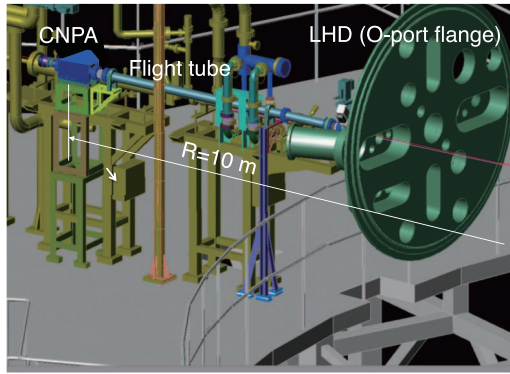


Fig. 2 Three-dimensional illustration of the CNPA on LHD. The CNPA is installed on the diagnostic platform and connected to the O-port.

tron array.

CNPA is installed on the diagnostic platform and connected to the outside horizontal port (O-port) via a flight tube. A 3-dimensional view of CNPA without the neutron shield is shown in Fig. 2. In LHD, CNPA measures the radial high energy particle distribution combining with the impurity pellet measurement.

### 3. Radiation Environment Around LHD

The special distribution and the energy spectra of neutrons and gamma-rays in the LHD torus hall have been calculated by a General Monte Carlo N-Particle Transport Code version 6 (MCNP-6) [5] with the nuclear data library of ENDF/B-VII.1 [6], where LHD and the LHD experimental building are modeled manually based on the CAD drawings [7]. The schematic view of the MCNP calculation model is shown in Fig. 3, which is drawn by Super MC [8]. In the torus hall, the LHD and the interferometer support are modeled. The other apparatuses such as neutral beam injectors and vacuum pumps, are not included. Detailed modeling of LHD itself is described in Ref. [8, 9]. The source neutron energy is assumed to be 99.5% of 2.45 MeV and 0.5% of 14.1 MeV. The 14.1 MeV neutron is generated by the triton burnup process [10].

Figure 4 shows neutron and gamma-ray spectra on the center line of the O-port with several radial distances from the center of the torus for the maximum neutron emission rate of  $1.9 \times 10^{16}$  n/s. Virgin neutrons of 2.45 MeV and 14.1 MeV are clearly seen not only in the torus hall. It can be considered that several peaks and gaps in the keV region are corresponding to resonances of  $^{56}\text{Fe}$  and other structural materials. The thermal neutron peak is formatted in all spectra. There is not significant difference in the neutron flux and spectrum among the major radii of 10, 15 and 20 m in the torus hall. This is due to the reflection effect of the concrete wall.

In the gamma-ray spectra, prompt gamma-rays from concrete components, such as  $\text{H}(n, \gamma)$ ,  $^{56}\text{Fe}(n, n')$ ,  $^{29}\text{Si}(n, \gamma)$ , and  $^{56}\text{Fe}(n, \gamma)$  are identified. Also, there is not a large

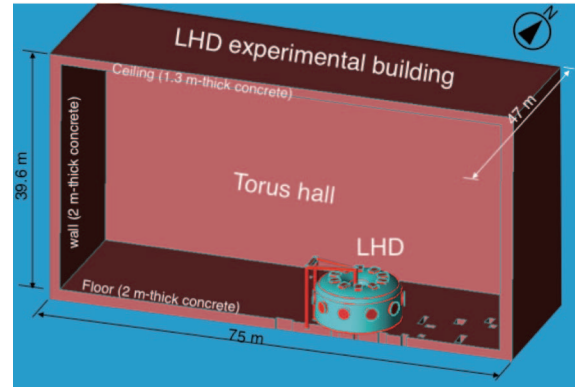


Fig. 3 Schematic view of the MCNP calculation model for LHD and the experimental building.

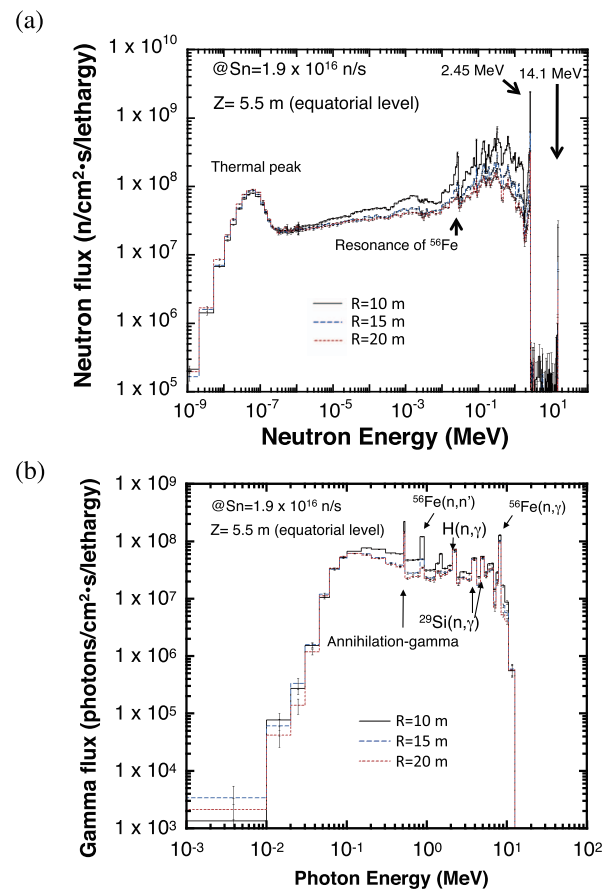


Fig. 4 (a) Neutron and (b) gamma-ray spectra at the neutron emission rate of  $1.9 \times 10^{16}$  n/s in the torus hall on the equatorial port (O-port) level ( $Z = 5.5$  m).

difference in the gamma-ray flux and spectrum among the major radius of 10, 15 and 20 m.

### 4. Neutronics Analyses of the CNPA Shield

#### 4.1 Analyses of the original shield

A photograph of the original shield made of 15 cm thick borated polyethylene is shown in Fig. 5. The original

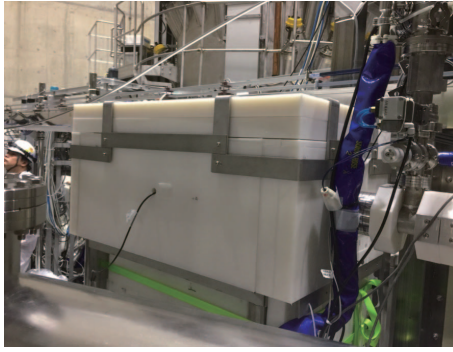


Fig. 5 Photograph of the original shield for the CNPA.

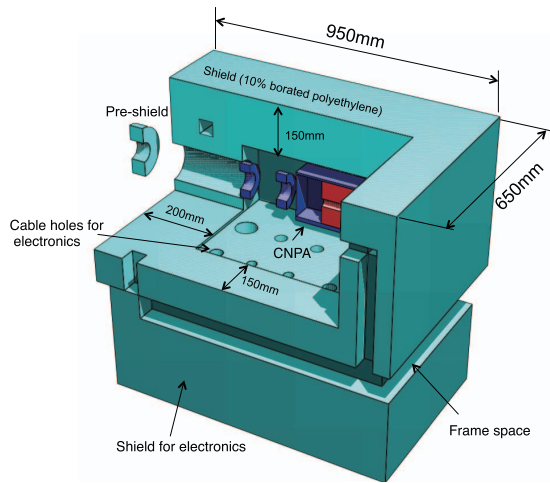


Fig. 6 MCNP calculation model of the original shield for CNPA. Frame of stainless steel is modeled, but not shown in this figure.

shield is based on the preliminary neutronics design [9], but is not the same as the preliminary neutronics design itself. In the preliminary shielding design, the shield is modeled by a simple box of borated polyethylene. However, the original shield has a detailed structure such as cable holes and support frames. Also, a shield for electronics is added under the main shield for the CNPA.

As described above, this shield is insufficient for higher neutron yield plasma shots. At first, neutronics analysis is carried out for the original shield taking into account such detailed structures. The original shield is modeled as precise as possible for the MCNP calculation as shown in Fig. 6.

In order to identify the neutron and gamma-ray transport roots to the detectors of CNPA, we carried out the neutronics calculations for three models: the original shield, the original model without cable holes, and the original model without cable holes and the beam inlet. In the MCNP calculations, these three models of the CNPA are incorporated with the LHD whole model shown in Fig. 3. In order to improve the statistics of the calculation, the grid mesh type weight window technique is employed. The typical number of source particles is  $5 \times 10^8$ . Figures 7

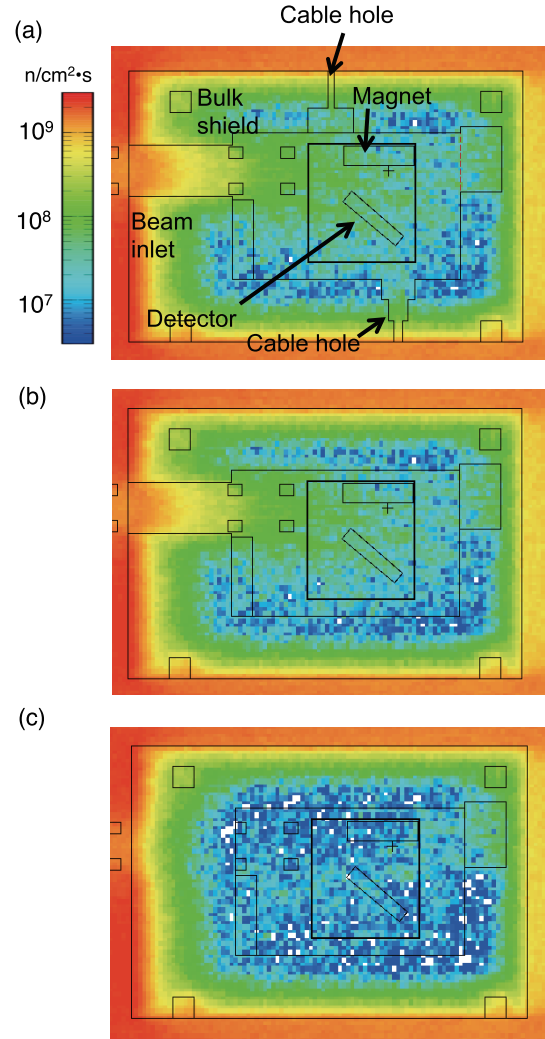


Fig. 7 Neutron flux distribution on the horizontal plane in the CNPA at the neutron emission rate of the neutron emission rate of  $1.9 \times 10^{16}$  n/s for (a) the original shield, (b) without cable holes, and (c) without cable holes and the beam inlet hole.

Table 1 Neutron and gamma-ray flux at the detector position in the CNPA for the neutron emission rate of  $1.9 \times 10^{16}$  n/s.

Flux (n/cm <sup>2</sup> ·s)	Original shield	w/o cable holes	w/o cable holes and beam inlet
Neutrons	$2.6 \times 10^7$	$2.4 \times 10^7$	$1.0 \times 10^7$
Gamma-rays	$3.5 \times 10^8$	$3.5 \times 10^8$	$3.4 \times 10^8$

and 8 show calculated neutron and gamma-ray distributions, respectively, in the CNPA on the horizontal plane at the neutron emission rate of the neutron emission rate of  $1.9 \times 10^{16}$  n/s for those three models. Also, Table 1 summarized neutron and gamma-ray flux at the detector position at the neutron emission rate of  $1.9 \times 10^{16}$  n/s for those three models.

The neutron streaming from the cable holes is not significant contribution to the neutron flux at the detectors. On

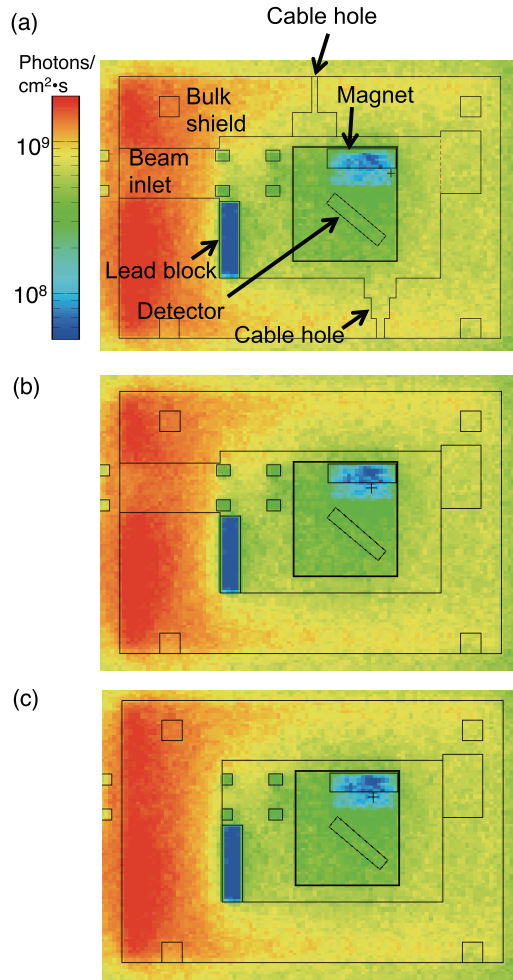


Fig. 8 Gamma-ray flux distribution in the CNPA at the neutron emission rate of  $1.9 \times 10^{16}$  n/s for (a) the original shield, (b) without cable holes, and (c) without cable holes and the beam inlet hole.

other hand, the contribution of neutron streaming from the beam inlet is approximately 60% to the neutron flux at the detector position. Therefore, reducing the beam inlet diameter is very effective for reducing the neutron flux at the detector position. Even though we close cable holes and the beam inlet, the neutron flux at the detector position is still  $1.0 \times 10^7$  n/cm²·s, which is the contribution from the neutron transmission through the bulk shield. Therefore, adding the bulk shield thickness is also required to reduce the neutron flux at the detector position in order to be lower than  $1 \times 10^7$  n/cm²·s.

There is no significant difference of the gamma-ray flux at the detector position among those three models. Gamma-rays are generated inside the bulk shield near the surface facing to LHD. However, generated gamma-rays are absorbed by the bulk shield itself. We installed a lead block to protect the detectors from the gamma-rays generated inside the bulk shield. However, it seems that the lead block is not effective for reducing the gamma-ray flux at the detector position.

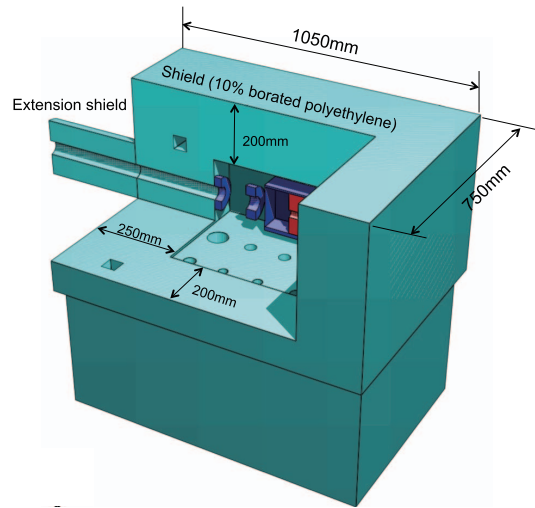


Fig. 9 MCNP calculation model of the upgraded shield for the CNPA.

## 4.2 Upgraded shield and the analysis

By the neutronics analyses for the original shield, we carried out the design of the upgrade shield as shown in Fig. 9. The borated polyethylene with 5 cm thickness is added to the bulk shield. The diameter of the beam inlet is reduced from 124 mm to 65 mm. Furthermore, an extension shield of 20 cm in diameter and 35 cm in length is added at the beam inlet. The neutron streaming from the cable holes is not significant. However, the cable holes will be filled with plastic putty to enhance the shielding performance. The thickness of the plastic putty is assumed to be equivalent to the 5 cm polyethylene in the neutronics analysis.

The MCNP calculation is performed for the upgrade shield for the CNPA shown in Fig. 9. Figures 10 and 11 show neutron and gamma-ray distributions in the CNPA at the neutron emission rate of  $1.9 \times 10^{16}$  n/s for the upgraded shield on horizontal and vertical planes. It is clearly observed that the neutron flux at CNPA is reduced remarkably. The neutron flux at the detector position is  $1.9 \times 10^6$  n/cm²·s, which is low enough for the required specifications. Also, the gamma-ray flux at the detector position is  $2.6 \times 10^8$  n/cm²·s, which is approximately 2/3 of that of the original shield.

Figure 12 shows neutron and gamma-ray spectra at the detector position in the CNPA. In the neutron spectrum, virgin neutrons of 2.45 MeV and the flat spectrum generated by the slowing down process are clearly seen. In these calculations, the source neutron energy in the plasma is assumed to be 2.45 MeV only. The 14 MeV source neutron is not taken into account, because the fraction of the 14 MeV source neutron is typically 0.1-0.2% of the total neutron in many shots of the first deuterium plasma campaign. Because the boron in the borated polyethylene absorbs thermal neutrons, the thermal peak lower than 0.1 eV is not observed.



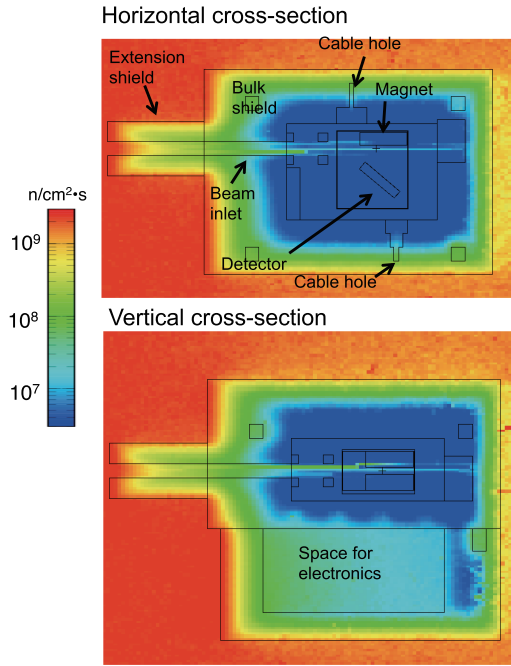


Fig. 10 Neutron flux distribution on the horizontal and vertical planes in CNPA at the neutron emission rate of the neutron emission rate of  $1.9 \times 10^{16}$  n/s.

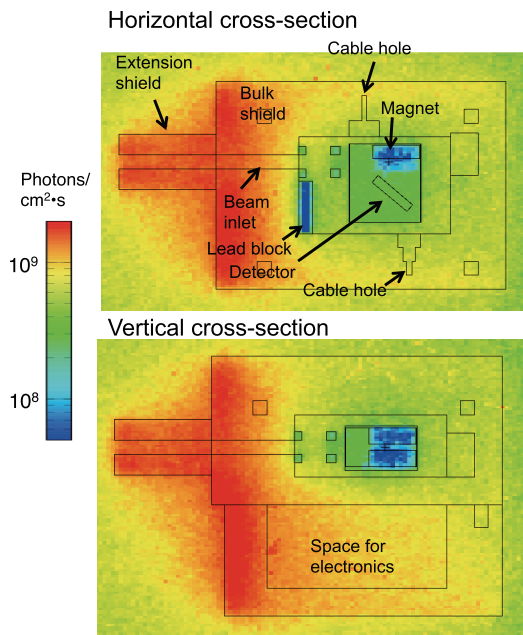


Fig. 11 Gamma-ray flux distribution on the horizontal and vertical planes in CNPA at the neutron emission rate of the neutron emission rate of  $1.9 \times 10^{16}$  n/s.

The gamma-ray spectrum is softer than that of the environment in the torus hall shown in Fig. 4 (b). In the CNPA, gamma-rays lower than 0.5 MeV are dominant. The prompt gamma-rays from neutron capture reactions of  $^{56}\text{Fe}(n, \gamma)^{57}\text{Fe}$ ,  $\text{H}(n, \gamma)\text{D}$  and annihilation gamma-rays of 0.511 MeV are identified. There is no guide line of

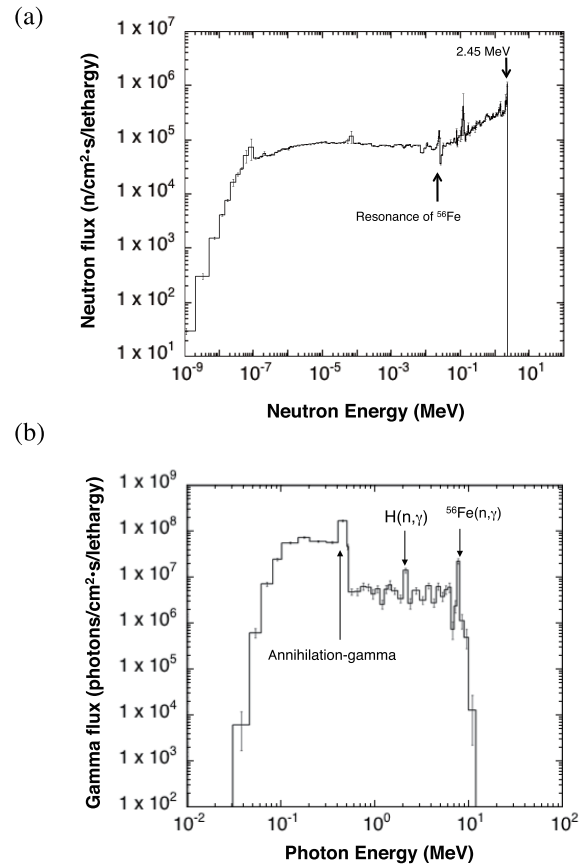


Fig. 12 (a) Neutron and (b) gamma-ray spectra at the detector position in CNPA for the neutron emission rate of  $1.9 \times 10^{16}$  n/s.

the gamma-ray effect on the channeltron. However, the gamma-ray may generate secondary electrons on the active area of the channeltron. Therefore, it is considered that gamma-rays also will make noises in the CNPA measurement. Gamma-rays lower than 0.5 MeV are relatively shielded easily by a tungsten sheet or similar material. It is proposed that the channeltron detector array should be covered by the tungsten sheet locally.

## 5. Summary

Neutronics design for the upgraded shield of CNPA has been performed using the MCNP6 code to prevent the neutron-induced noise in the higher neutron emission rate shots of LHD. At first, we carried out the detailed neutronics analyses for the original shield with taking account of the detailed structure such as cabling holes and support frames in order to identify the neutron transport root to the detectors. It is found that contributions of the neutron streaming from the beam inlet and the penetration of the bulk shield are approximately 60% and 40%. Consequently, 5 cm borated polyethylene plates are added to the bulk shield and the borated polyethylene cylinder shield of 20 cm in diameter and 35 cm in length is added around the flight tube. In the upgraded shield, the neutron flux is

expected to be  $1.7 \times 10^6$  n/cm<sup>2</sup>·s at the detector array at the neutron emission rate of  $1.9 \times 10^{16}$  n/s, which is low enough for the required specifications.

## Acknowledgments

This work was supported by the LHD project budgets (ULHH003 and ULGG801).

- [1] M. Osakabe *et al.* Fusion Sci. Technol. **72**, 199 (2018).
- [2] M. Osakabe *et al.*, IEEE Trans. Plasma Sci. **46**, 2324 (2018).
- [3] T. Ozaki *et al.*, Rev. Sci. Instrum. **79**, 10E518 (2008).
- [4] Ioffe institute, *Neutral particle analyzer*, <http://www.ioffe.ru/ACPL/npd/npa00.htm>
- [5] D.B. Pelowitz (Ed.), *MCNP6 users Manual*, LA-CP-13-00634, Los Alamos National Laboratory (2013).
- [6] M.B. Chadwick *et al.*, Nucl. Data Sheets **112**, 2887 (2011).
- [7] T. Nishitani *et al.*, Fusion Eng. Des. **123**, 1020 (2017).
- [8] Y. Wu *et al.*, Fusion Eng. Des. **84**, 1987 (2009).
- [9] T. Nishitani *et al.*, forthcoming in Progress in Nucl. Sci. Technol.
- [10] M. Isobe *et al.*, IEEE Trans. Plasma Sci. **46**, 2050 (2018).